States of Light Nuclei from the jj Coupling Model*

D. KURATH
Argonne National Laboratory, Chicago, Illinois
(Received July 17, 1952)

The ordering of energy levels is presented for $1p$ shell nuclei in the jj coupling model. Comparison of the jj and LS model predictions with experiment are given for angular momenta and magnetic moments of the ground states as well as for the shape of the binding energy curve. No decisive favoring of either model is evident.

INTRODUCTION

THE ordering of energy levels for nuclei in the $1p$ shell, which extends from He^4 to O^{16}, has been investigated by Feenberg and Wigner[1] and Feenberg and Phillips.[2] These authors performed a Hartree method calculation under the assumption that spin-orbit coupling forces are negligibly small. As a result the orbital angular momenta of the individual nucleons $\mathbf{l}_i$ are coupled to give the total angular momentum $\mathbf{L}$ of the nucleus as a good quantum number. The same holds for the individual spins $\mathbf{s}_i$ and the total spin $\mathbf{S}$, so the model is referred to as the LS coupling model.

In the present calculation the opposite assumption is made about spin-orbit forces, namely, that they are large. As a result the individual nucleon $\mathbf{l}$ and $\mathbf{s}$ are coupled to give a resultant angular momentum $\mathbf{j}$. The $\mathbf{j}_i$ are then coupled to give the total angular momentum $\mathbf{I}$ of the nucleus. A Hartree method calculation is carried out for this, the jj coupling model of the nucleus, and the results are presented in a form that facilitates comparison with the earlier calculation for the LS model.

PROCEDURE

In both models each individual particle is assumed to move in a central potential well representing the average effect of the other nucleons. For the jj model there is assumed to be an additional term in the potential, proportional to $\mathbf{l}_i \cdot \mathbf{s}_i$, which couples the spin and orbital angular momentum for each individual particle to give it total angular momentum $j=l\pm\frac{1}{2}$. The sign of this single-particle coupling term is chosen to give the state $1p_{\frac{3}{2}}$ lower in energy than the state $1p_{\frac{1}{2}}$, and the contribution of spin-orbit coupling to the potential energy for a configuration of nucleons is then an additive term depending solely on the number of nucleons present in each shell. The $1p$ shell is thereby split into two parts, the region from He^4 to C^{12} consisting of configurations of $1p_{\frac{3}{2}}$ nucleons, while from C^{12} to O^{16} the $1p_{\frac{1}{2}}$ nucleons are filled in.

The radial dependence of the individual particle function is chosen to be that of a three-dimensional harmonic oscillator, namely,

$$R_p = N_p r \exp[-(r/r_p)^2].$$

The attractive forces acting between nucleons are assumed to be charge independent and sufficiently greater than the Coulomb repulsion of the protons so that the isotopic spin T is a good quantum number. In the Hartree approximation the nuclear wave function is represented by a function consisting of products of individual particle functions. These product functions are then made antisymmetric to the complete exchange of any two nucleons, and the further stipulation of total angular momentum I and isotopic spin T serves to determine the wave function uniquely for all but one nuclear configuration.[3] The splitting of the energy levels under various interactions is then calculated as a first-order perturbation using the wave functions determined in the above manner as zero-order functions.

The potential energy of interaction of the $1p$ shell nucleons, exclusive of the Coulomb contribution, is the term that determines the separation of the possible levels for each nucleus. Matrix elements are calculated for the four possible types of exchange[4] that represent the general interaction under restriction to a static central-force potential:

$$V_{12} = [1 \text{ or } P_{12} \text{ or } Q_{12} \text{ or } P_{12}Q_{12}]J(r_{12}), \qquad (1)$$

where P_{12} and Q_{12} are, respectively, space and spin exchange of particles 1 and 2. These types of exchange in the order in which they appear in Eq. (1) are customarily called Wigner, Majorana, Bartlett, and Heisenberg interactions. The range dependence used is the negative Gaussian $J(r_{12}) = A \exp[-(r_{12}/r_0)^2]$. The matrix elements are given in terms of the same integrals L and K, which are defined in reference 1. In terms of the parameters present in $J(r_{12})$ and R_p the integrals are

$$\begin{aligned} K &= \tfrac{1}{4}A(r_p/r_0)^4[1+(r_p/r_0)^2]^{-7/2}, \\ L/K &= 3+4(r_0/r_p)^4[1+(r_p/r_0)^2]. \end{aligned} \qquad (2)$$

The contributions to the potential energy due to $1p$ shell interactions are given for the various nuclei in Table I. For nuclei between He^4 and C^{12} the table

* Work done in part at the University of Chicago, Chicago, Illinois.

[1] E. Feenberg and E. Wigner, Phys. Rev. **51**, 95 (1937).

[2] E. Feenberg and M. Phillips, Phys. Rev. **51**, 597 (1937).

[3] The two states of $I=2$, $T=0$ in Be^8 must be resolved by solution of a secular equation.

[4] E. Wigner and L. Eisenbud, Proc. Natl. Acad. Sci. **27**, 281 (1941).

TABLE I. Matrix elements and quantum numbers for the potential energy of interaction in the $1p$ shell.

Nucleus	State I	State T	Matrix elements all have factor 1/9 P_{12}	1	$P_{12}Q_{12}$	Q_{12}
He^6	2	1	$-3L+15K$	$9L-21K$	$-9L+21K$	$3L-15K$
	0	1	$3L+21K$	$9L+3K$	$-9L-3K$	$-3L-21K$
Li^6	3	0	$9L-9K$	$9L-9K$	$9L-9K$	$9L-9K$
	2	1	$-3L+15K$	$9L-21K$	$-9L+21K$	$3L-15K$
	1	0	$-L+21K$	$9L-9K$	$9L-9K$	$-L+21K$
	0	1	$3L+21K$	$9L+3K$	$-9L-3K$	$-3L-21K$
Li^7, Be^7	7/2	1/2	$9L+9K$	$27L-45K$	$18K$	$18L-36K$
	5/2	1/2	$2L+30K$	$27L-45K$	$18K$	$11L-15K$
	3/2	3/2	$-6L+48K$	$27L-51K$	$-27L+51K$	$6L-48K$
	3/2	1/2	$12L+30K$	$27L-15K$	$-12K$	$6L-30K$
	1/2	1/2	$-6L+54K$	$27L-45K$	$18K$	$3L+9K$
Li^8	3	1	$6L+54K$	$54L-90K$	$-18L+54K$	$24L-72K$
	2	1	$6L+66K$	$54L-78K$	$-18L+42K$	$18L-66K$
	1	1	$-4L+84K$	$54L-90K$	$-18L+54K$	$14L-42K$
	0	2	$-12L+96K$	$54L-102K$	$-54L+102K$	$12L-96K$
Be^8	4	0	$14L+30K$	$54L-90K$	$36K$	$32L-60K$
	3	1	$6L+54K$	$54L-90K$	$-18L+54K$	$24L-72K$
	2	1	$6L+66K$	$54L-78K$	$-18L+42K$	$18L-66K$
	2	0	$72K$	$54L-90K$	$36K$	$18L-18K$
	2	0	$18L+54K$	$54L-54K$	0	$18L-54K$
	1	1	$-4L+84K$	$54L-90K$	$-18L+54K$	$14L-42K$
	0	2	$-12L+96K$	$54L-102K$	$-54L+102K$	$12L-96K$
	0	0	$24L+60K$	$54L-30K$	$-24K$	$12L-60K$
Be^9, B^9	7/2	1/2	$15L+81K$	$90L-144K$	$-18L+72K$	$42L-108K$
	5/2	1/2	$8L+102K$	$90L-144K$	$-18L+72K$	$35L-87K$
	3/2	3/2	$120K$	$90L-150K$	$-45L+105K$	$30L-120K$
	3/2	1/2	$18L+102K$	$90L-114K$	$-18L+42K$	$30L-102K$
	1/2	1/2	$126K$	$90L-144K$	$-18L+72K$	$27L-63K$
B^{10}	3	0	$21L+135K$	$135L-207K$	$-27L+99K$	$57L-153K$
	2	1	$9L+159K$	$135L-219K$	$-45L+129K$	$51L-159K$
	1	0	$11L+165K$	$135L-207K$	$-27L+99K$	$47L-123K$
	0	1	$15L+165K$	$135L-195K$	$-45L+105K$	$45L-165K$
Be^{10}, C^{10}	2	1	$9L+159K$	$135L-219K$	$-45L+129K$	$51L-159K$
	0	1	$15L+165K$	$135L-195K$	$-45L+105K$	$45L-165K$
B^{11}, C^{11}	3/2	1/2	$18L+216K$	$189L-297K$	$-54L+162K$	$72L-216K$
C^{12}	0	0	$24L+288K$	$252L-396K$	$-72L+216K$	$96L-288K$
B^{12}, N^{12}	2	1	$24L+273K$	$252L-411K$	$-90L+258K$	$90L-282K$
	1	1	$16L+297K$	$252L-411K$	$-90L+270K$	$94L-282K$
C^{13}, N^{13}	1/2	1/2	$30L+360K$	$324L-522K$	$-108L+324K$	$120L-360K$
N^{14}	1	0	$41L+432K$	$405L-660K$	$-135L+420K$	$149L-432K$
	0	1	$33L+456K$	$405L-660K$	$-153L+444K$	$147L-456K$
O^{14}, C^{14}	0	1	$33L+456K$	$405L-660K$	$-153L+444K$	$147L-456K$
O^{15}, N^{15}	1/2	1/2	$45L+540K$	$495L-810K$	$-180L+540K$	$180L-540K$
O^{16}	0	0	$54L+648K$	$594L-972K$	$-216L+648K$	$216L-648K$

includes only configurations of $p_{\frac{3}{2}}$ nucleons. Such configurations should provide the low-lying levels, but when the excitation energy is more than about 2 Mev, nuclei in this region may have excited levels given by configurations of mixed $p_{\frac{3}{2}}$ and $p_{\frac{1}{2}}$ nucleons. The mixed configurations are not included in the table. The table can be compared with that constructed for the LS coupling model;[2] the values $K=0.82$ Mev and $L=5.63$ Mev used in that calculation provide reasonable orders of magnitude for numerical evaluation.

1. Nuclear Spins and Magnetic Moments

The singlet-triplet potential difference of the deuteron, as determined from low energy neutron-proton scattering, indicates that the central potential interaction has a weight of about 0.80 for space dependence (1 and P_{12}) and about 0.20 for spin dependence (Q_{12} and $P_{12}Q_{12}$). Table II gives the experimental nuclear spins as well as the spins of the ground states obtained from the two models with a potential whose space dependence is predominantly P_{12} and with nuclear parameters such that $4<L/K<9$. The observed magnetic moments, together with calculated values for each case where a model gives the correct ground state spin, are also included. Even-even nuclei are not included since all results give a spin of zero for the ground states.

The models are both in agreement with the experimental spins for all the nuclei except Li^6, B^{10}, B^{11}, and B^{12}. The LS model gives the experimentally observed value of 1 for the spin of Li^6, and the magnetic moment calculated from this ground state[5] is much closer to the experimental moment than that obtained[6] from the jj model state of spin 1 ($\mu=0.63$ nm). However, for B^{10} the situation is reversed and only the jj model gives the measured spin of 3 as well as a good value for the magnetic moment.[7] For B^{11} the observed spin of $\frac{3}{2}$ is given correctly by the jj model, while the LS model predicts the state $^2P_{\frac{1}{2}}$. In order to have an allowed beta-decay from B^{12} to the C^{12} ground state (spin zero), the spin of B^{12} should be 0 or 1. This can be obtained from the LS model, but the jj model gives a spin of 2 unless $L<3.5K$ which is not likely.

From the magnetic moments listed in Table II, it is evident that in cases where both models give the experimental spin, the jj model usually gives a better value[8] for the magnetic moment. For nuclei in this category the jj values are within 10 percent of the experimental values. The cases in which the spin predictions disagree include the previously discussed Li^6 and B^{10} plus B^{11}. In B^{11} the spin is given correctly by the jj model, but the calculated magnetic moment is considerably larger

TABLE II. Ground-state nuclear spins and magnetic moments.

Nucleus	Nuclear spins Exp	LS	jj	Magnetic moments (Nuclear magnetons) Exp	LS[a]	jj[b]
Li^6	1	1	3	0.822	0.88	···
Li^7	3/2	3/2	3/2	3.257	3.10	3.03
Li^8	(2)[c]	2	2			
Be^9	3/2	3/2	3/2	−1.178	−1.56	−1.15
B^{10}	3	1	3	1.801	···	1.88
B^{11}	3/2	1/2	3/2	2.689	···	3.79
B^{12}	(1 or 0)[c]	1 or 0	2			
C^{13}	1/2	1/2	1/2	0.702	1.10	0.64
N^{14}	1	1	1	0.404	0.88	0.37
N^{15}	1/2	1/2	1/2	−0.283	−0.26	−0.26

[a] Values of reference 5 corrected for the present values of $\mu_p=2.79$ and $\mu_n=-1.91$ nuclear magnetons.
[b] E. Feenberg, Phys. Rev. **76**, 1275 (1949); M. Mizushima and M. Umezawa, Phys. Rev. **85**, 37 (1952); these contain most of the jj calculations.
[c] Inferred from beta-decay.

[5] M. E. Rose and H. A. Bethe, Phys. Rev. **51**, 205 and 993 (1937).
[6] M. G. Mayer, Phys. Rev. **78**, 16 (1950).
[7] Feenberg and Phillips have suggested (see reference 2) that the ground state of the LS model is a ^3D due to repulsion of two low-lying ^3D states. However, since spin-orbit coupling does not split the $^3D_{3,2,1}$ states, it is not evident that the ground state of B^{10} should be 3.
[8] The LS value for N^{14} in Table II is for the $^3S_1$ ground state. It has been suggested in reference 2 that the ground state is really $^3D_1$, which has a magnetic moment of 0.31 nm.

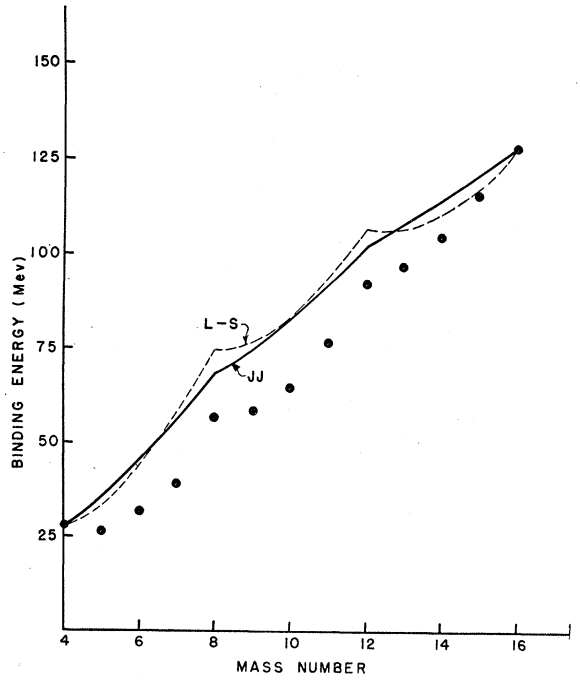

FIG. 1. Binding energy as function of mass number for the $1p$ shell. The curves for the LS model and the jj model are given under the assumption that the integrals L and K are independent of mass number. Circles are experimental points.

than observed. The LS state, $^2P_{\frac{3}{2}}$, gives a moment of 3.44 nm which is somewhat smaller than the jj value but still considerably larger than experiment, which leaves B^{11} as the only nucleus for which neither model comes close to the observed moment.

The general conclusion from comparison of spins and magnetic moments with experiment is that both models give a considerable amount of agreement. However, for the points wherein they disagree neither model is favored consistently by the experimental results.

2. Energy Comparisons

Futher tests for the models are provided by the experimental isobar differences and by the structure of the experimental binding energy curve for stable nuclei. The points for comparison of the models are three:

(A) The isobar differences for mirror nuclei, which depend only on a Coulomb term, and are thus independent of the interaction integrals L and K, but do depend on the parameter r_p in the oscillator wave function.

(B) The four-shell structure in the binding energy curve, whose features depend on the type of interaction among the p-shell nucleons and also depend on the magnitude of the integrals L and K.

(C) The isobar differences between odd-odd and even-even nuclei, which involve the interaction integrals L and K as well as a Coulomb term.

(A) *Mirror Isobars*

For these isobars the difference in binding energy is obtained from the electrostatic repulsion of p-shell protons by the s-shell protons plus the matrix elements for Coulomb interaction of p-shell protons with each other. Only the latter contribution is dissimilar for the jj model and LS model calculations. The matrix elements from the LS model are given in Table IV of reference 2 in terms of the Coulomb integrals L_c and K_c. However, since[1] $L_c=49/3\ K_c$, the value is determined largely by the L_c term which is the same for all isotopes of a given element. Therefore, the matrix elements agree within a few percent for the ground states of all nuclei having the same Z. In terms of the value for the Be^7 ground state in LS coupling C, defined as $C=L_c+2/3K_c=17K_c$, the matrix elements are given in Table III for the two models. It is apparent that the Coulomb matrix elements are nearly identical for the two models, so that for the mirror isobars the calculated binding energy differences are substantially the same. The constants used in the LS calculation[1,2] give $C=0.47$ Mev and for the interaction of a p-shell proton with the two s-shell protons, $C_{sp}=0.84$ Mev. These numbers result in theoretical values for the nine mirrors that are about 20 percent to 30 percent lower than the experimental values. This point will be discussed in Sec. C.

B. Binding Energy Curve

The total binding energy as calculated with Hartree wave functions has a very unsatisfactory magnitude, a failing that is attributed to the limitations of such product-form wave functions. However, the potential energy of interaction within the p-shell, including the Coulomb term, superimposes a structure on the general trend of the binding energy curve. This can be compared for the two models with the structure evident in the experimental curve.

The experimental binding energy curve of the most tightly bound nuclei at each mass number has maxima at He^4, Be^8, C^{12}, and O^{16} with pronounced dips between the peaks which become shallower with increasing mass number. Of the four static central-force interactions in Table I, only the P_{12} (Majorana) type presents a comparable structure.[9] Since this is true for both models,

TABLE III. Coulomb matrix elements within the p-shell.

Element	LS model	jj model
Be	C	$0.95C$
B	$2.60C$	$2.55C$
C	$5.25C$	$5.10C$
N	$8.45C$	$8.45C$
O	$12.65C$	$12.65C$

[9] Wigner interaction does have the type of four-structure desired in the limit of vanishing range of interaction where Majorana and Wigner interactions become identical. However, for the ranges expected physically the Wigner four-structure is very slight.

the Majorana term should be dominant in the interaction. The degree to which the four-structure is accented depends on the exact interaction used, and also it depends quite strongly on the ratio L/K. The LS model contains the possibility of having very pronounced four-structure, but the jj model suppresses this feature to a large extent. While there is a peak at $A=8$ in the jj model, the peak at $A=12$ is due almost wholely to the spin-orbit coupling term which is assumed to contribute about $+2$ Mev of binding energy for every $p_{\frac{3}{2}}$ nucleon and -4 Mev for every $p_{\frac{1}{2}}$ nucleon, the $p_{\frac{1}{2}}$ shell coming above C^{12}. As an example of the comparative amount of four-structure available from the models, the calculated binding energies, fitted at He^4 and O^{16} by adding a linear amount of binding as in the previous LS calculation, are given in Fig. 1. The particular interaction is $V_{12}=(0.8\,P_{12}+0.2\,P_{12}Q_{12})J(r_{12})$, with the numerical values $L=5.63$ Mev and $K=0.82$ Mev. The dips between peaks of binding energy are much deeper for the LS model than for the jj model. However, they tend to become more pronounced with increasing A in the LS model which is contrary to the experimental result. This behavior is probably due to the fact that L and K were assumed constant throughout the p shell. From their dependence on the oscillator parameter r_p, which is related to the size of the nucleus, one would expect them to decrease considerably between $A=4$ and 16, giving decreased four-structure at larger A. Assuming that r_p is proportional to $A^{\frac{1}{3}}$ and that $L=5.63$ Mev and $K=0.82$ Mev at He^4 leads one to the curves in Fig. 2 which have a behavior much more similar to the experimental one than those of Fig. 1.

Quantitative comparisons are on speculative ground, owing to lack of knowledge of the nuclear interaction, the uncertainty in the nuclear parameters, and the use of Hartree wave functions. However, the conclusion can be drawn that LS coupling is indicated by the shape of the experimental binding energy curve, certainly for the lower half of the shell. While the jj model could give reasonable agreement for the heavier nuclei by using a larger L/K ratio, it would then fit the light nuclei rather poorly.

The source of the four-structure in the LS model has been pointed out to be the symmetry structure of the spatial part of the wave functions. Maximum symmetry and maximum binding energy for Majorana interaction occur simultaneously whenever a group of four is completed. The suppression of the four-structure by the jj model is due to the fact that the spin-orbit coupling mixes states of different spatial symmetry properties and thus destroys the structure to a large extent. Hence for the light nuclei, jj coupling does not seem likely.

C. *Even-Even and Odd-Odd Isobars*

The differences in binding energy between even-even and odd-odd isobars involve a Coulomb term plus a term involving L and K. These isobars occur at mass numbers 6, 8, 10, 12, and 14 which involve most of the points where one or the other model gives a spin differing from the observed value. In view of the uncertainties in the interaction and nuclear constants it does not seem feasible to attempt a quantitative comparison. In the earlier LS calculation, a fair agreement with four-structure and these isobar differences was obtained at the expense of using nuclear parameters that give differences for mirror isobars lying from 20 percent to 30 percent lower than observation, as mentioned before. The use of these nuclear parameters for the cases where the spin is obtained correctly in the jj model gives differences between even-even and odd-odd isobars that have the same order of magnitude as the LS results, although the agreement with experimental values is not as good. However, the uncertainties mentioned above plus the fact that the Coulomb term cannot be simultaneously satisfied with the parameters used make quantitative comparison for this group of isobars a rather dubious test.

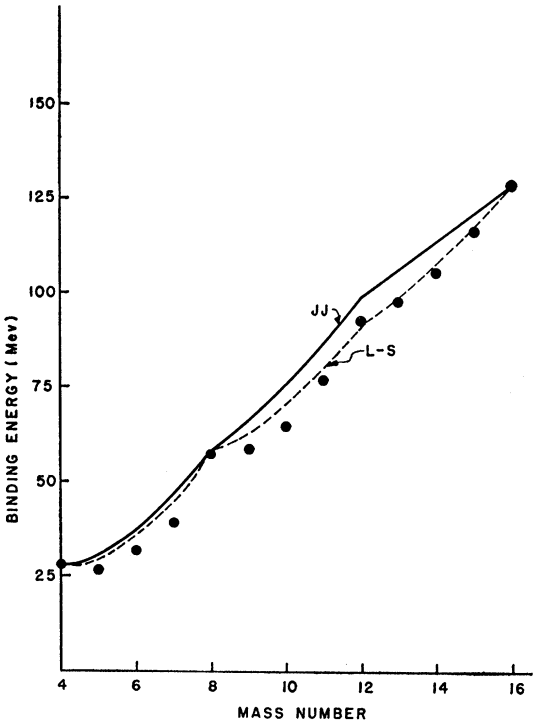

FIG. 2. Binding energy as functions of mass number A under the assumption that the oscillator parameter r_p is proportional to $A^{\frac{1}{3}}$. Circles are experimental points.

CONCLUSIONS

In so far as the Hartree method is used in both models, it would not be expected that the quantitative separation of levels is given correctly. However, the approximation should be good enough to give the order of levels and the relative binding for neighboring nuclei.

In this respect the calculation should serve for comparison of the hypotheses of weak or strong spin-orbit coupling. The chief points for comparison of the models are the angular momenta (spins) and magnetic moments of the ground states and the four-shell structure of the binding energy curve. In comparing the spins with experiment both models give some incorrect values, and neither is to be preferred over the other. The magnetic moments are generally somewhat better for the jj model. From the binding energy curve, the LS model seems preferable since it contains a pronounced four-structure. It is possible that there is a transition from LS coupling in the early part of the shell to jj coupling in the latter part, which would remove most of the spin difficulties and not affect the binding energies seriously. The present influx of experimental data on energy levels of the $1p$-shell nuclei should help greatly to clarify the problem.

The author wishes to express his appreciation to Professor M. G. Mayer for discussion and guidance in the course of this work.

PHYSICAL REVIEW VOLUME 88, NUMBER 4 NOVEMBER 15, 1952

Electrostatic Analysis of Nuclear Reaction Energies. II*

D. S. Craig,† D. J. Donahue, and K. W. Jones
University of Wisconsin, Madison, Wisconsin

(Received July 29, 1952)

Electrostatic analysis of incident and product particle energies has been used to measure the following ground state Q-values: $O^{16}(d,\alpha)N^{14}$ (3.113±0.0035 Mev), $B^{10}(p,He^3)Be^8$ (−0.536±0.003 Mev), and $B^{10}(p,\alpha)Be^7$ (1.147±0.0025 Mev). The energy of the lowest level in B^{10} has been determined to be 719±1.6 kev; that of Be^7 to be 429±3 kev. Approximate cross sections are given for the above reactions and upper limits for $O^{16}(d,\alpha)N^{14*}$ (2.3-Mev level), and for $B^{10}(p,p')B^{10*}$ (2.1- and 1.7-Mev levels).

I. INTRODUCTION

FURTHER accurate measurements of nuclear Q-values have been made using the equipment and procedure described in earlier articles.[1,2] It will suffice here to say that a cylindrical electrostatic analyzer[3] was used for measuring the energy of the bombarding particles (T_1), and a spherical electrostatic analyzer[1] for measuring the energy of the product particles (T_2). A redetermination of the angle of observation with respect to the incoming beam, necessitated by a realignment of the spherical analyzer collimating apertures, was made using the measured positions of the apertures as described previously,[1] and by scattering deuterons from Li^6. The mean angle was found to be 134°33′±3′.

The nichrome resistor stack used in our earlier measurements was replaced with a new stack consisting of sixty one-megohm Shallcross Evenohm resistors, Type BX116E, whose temperature coefficient is less than 0.002 percent/°C. These were mounted with corona shields inside Lucite cylinders in which dried air was circulated by a blower. Several low voltage taps were provided to facilitate regulating and measuring the voltage over a wide range of values.

Several appendices are included with this paper. The first one consists of errata to paper I.[2] The second displays the form of the relativistic correction terms used in I and in II. The third appendix is concerned with the masses used in the calculations.

II. RESULTS AND DISCUSSION

$O^{16}(d,\alpha)N^{14}$

This Q-value is an important link in the group of reactions used by Li *et al.*,[4] in determining the masses of the light nuclei, as it is the only convenient connection to O^{16}, the standard of atomic masses.

Two determinations of this Q-value were made. The first was made using a target of 0.001-inch aluminum foil which had been heated in air to form the oxide. Because of the thickness of the aluminum it was impossible to scatter deuterons from the target in order to check the amount of contamination and the amount of oxygen. The observed counting rates of the doubly ionized alpha-particles are shown in Fig. 1. For a second run a target of beryllium oxide was prepared by heating in air a thick tantalum foil onto which had been evaporated beryllium. Since these targets were used immediately after putting them into the analyzer, it is reasonable to assume that the contamination on them is negligible. The rate at which carbon is deposited on a 1000A Ni foil was checked during the present measurements, and over a six-and-a-half-hour period of bombardment with a beam of the same magnitude as that used

* Supported by the Wisconsin Alumni Research Foundation and the AEC.

† Now with Atomic Energy of Canada, Ltd., Chalk River, Ontario, Canada.

[1] Browne, Craig, and Williamson, Rev. Sci. Instr. 22, 952 (1951).

[2] Williamson, Browne, Craig, and Donahue, Phys. Rev. 84, 731 (1951). This article will be referred to as I.

[3] Warren, Powell, and Herb, Rev. Sci. Instr. 18, 559 (1947).

[4] Li, Whaling, Fowler, and Lauritsen, Phys. Rev. 83, 512 (1951).